Evaluation of applied SFRC as a steel replacement in the design stage in a part of Cairo Metro line No. 4

Taher ELSAMNI, Nippon Civic Consulting Engineers Co. LTd., Tokyo, Japan, taher-el@nccnet.co.jp
Ashraf ABU-KRISHA, National Authority for Tunnels, Cairo, Egypt, ashamk66@hotmail.com
Takayoshi OTSUKA, Nippon Civic Consulting Engineers Co. LTd., Tokyo, Japan, otsuka@nccnet.co.jp
Kazuto FUJII, Nippon Civic Consulting Engineers Co. LTd., Tokyo, Japan, fujii@nccnet.co.jp

Topic: Planning and Designing Tunnels and Underground Structures

KEYWORDS: *Steel Fiber, lining, Tunnel, Concrete, Crack, Ductility*

1. Introduction

Apart from development in machine technology and other cross sectional tunnel shapes, the alternative lining systems. It has carried out as well, in early sixties in the former Soviet Republic experiments were carried out with tunnel lining without any joints [1] after excavation; the soil was replaced by in site poured concrete lining. At the end of the seventies and beginning of the eighties German and Japanese contractor’s further development the principle with idea to improve the following points [2]:

1 No secondary lining any more
2 Reducing the settlements
3 Improve the quality and behavior of the tunnel lining
4 Reduction of the construction cost by increase in construction speed
5 Developing the lining material. That which our aim of this technical paper

2. Paper aims and objectives

The main goal of this paper is to describe a design approach and evaluate the steel fiber reinforced segment for application in a part the underground of line No. 4, Cairo, Egypt. Background of the study that the Greater Cairo Metro line No. 4 phases 1 running from a depot/workshop via the Grand Egyptian Museum (GEM) to Elmalek Elsaleh Station with a length of 17.0 km, in a very dense sand soil, the designer propose to extend phase 1 by approximately 1.0km to solve some problem in the alignment and land acquisition, the area which is proposed to construct locate at the Muqattam Plateau, which is line stone, the cross section shown in Figure No.1. In addition, the feasibility study of phase 2 of the same line is almost rest in lime stone ground condition, that leads the designer to think of apply steel fiber reinforcement in the extended length which is about 600.0m. On the other hand, to reach a higher mechanical strength in terms of toughness, flexural and shear design stresses. Improved damage resistance during transportation and placing, improve durability in aggressive environments.

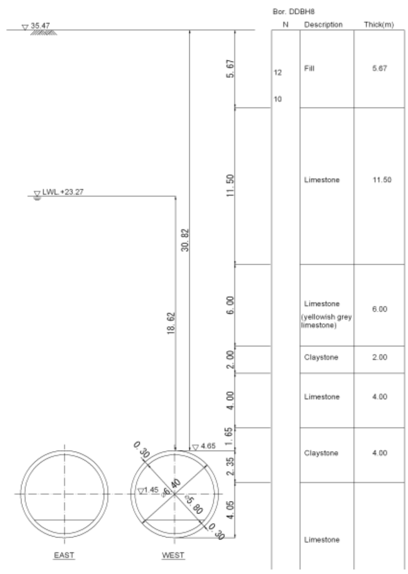

Figure 1: Tunnel through the Lime Stone Section 17k960m [1]

3. Design of section

3.1 The groundwater level

Fluctuations of Nile River; the maximum probable water level (17.33m), the minimum probable water level (15.55m) =1.8m, thus, the applied level in design is 25.07m-1.8m = 23.27m [1] .

3.2 Soil properties

Soil properties in the design are shown in the Table 1 [1], it is proposed to carry out design using nearest borehole data, which was carried out to collect soil layer information of cross section.

Table 1: Soil properties [1]

Soil layer	N value	Unit weight	Cohesion	Internal Friction angle	Young's modulus	Poisson's ratio
		γ(kN/m^3)	C (kN/m^2)	φ(°)	(kN/m^2)	
FILL	10	19.0	---	33.0	25,000	0.35
Top Clay	10	19.0	68	---	11,400	0.48
Sand1	37	19.0	---	37.0	92,500	0.35
Sand2	57	21.0	---	38.0	143,300	0.32
Sand3	100	22.0	---	41.0	250,000	0.30
Bottom Clay	63	19.0	269	---	37,400	0.45
Limestone (yellowish gray)	-	22.0	300	40.0	300,000	0.30
Limestone (Bluish gray)	-	23.0	300	40.0	300,000	0.30
Mudstone	-	22.0	100	30.0	150,000	0.40

4. Tunnel lining properties

- Segment lining, Type of segment reinforced concrete segment tenon type segment as shown in the Figure No. 2, outer diameter of segment lining=6.40 m, thickness of segment =0.3 m, width of segment =1.50 m, No. of Division of segment ring=6 (=3A-type+2B-type+K segment inserted in longitudinal direction), Concrete joint with inclined 2 bolts per joint, Elastic modulus of segment =3.15×107 kN/m^2
- Concrete specifications according to ECP203/2007, design basic strength f'_{ck} = 40 N/mm^2, Modulus of elasticity E_c = 31.5 kN/mm^2, sulphate resistance cement
- Normal black hooked steel fiber, L=30mm, diameter=0.5mm, Material satisfied the standard JIS G 3505[2], Mix rate of a steel fibre 0.4vol.%
- Shear spring constant between segment rings in Beam-spring model is calculated using the compressive rigidity of share strip material. Shear strip material is setting at ring joint. Figure 2, shows the details of shear strip position. Radial direction shear spring constant (k_{sr}) of this segment lining is k_{sr} = 34,500kN/m. For there is no restraint between segment rings, the tangential shear spring constant (k_{st}) of this segment lining is 0.0 kN/m.

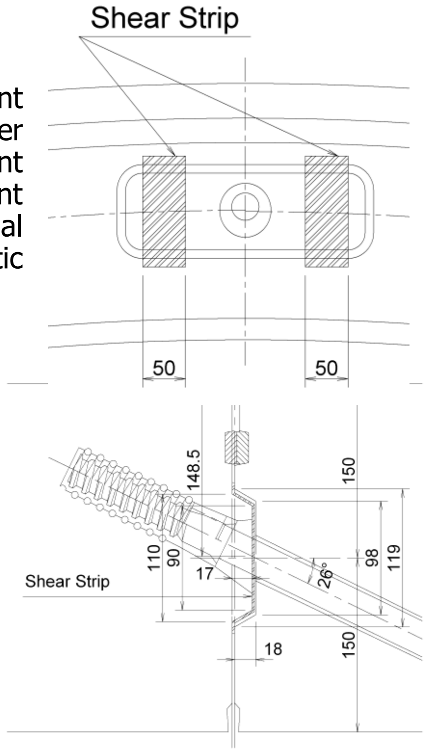

Figure 2: Ring joint of segment (Circumferential joint)

5. Loadings

Loadings of segment lining are carried out in accordance with the Standard Specifications for Tunneling [3]. Load combination between the earth pressures (effective stress method), dead weight of lining, effective of surcharge, soil reaction*, earthquake, effective of multiple parallel tunnel construction as shown in Figure 1, influence of vicinal construction, and the extra moment generated

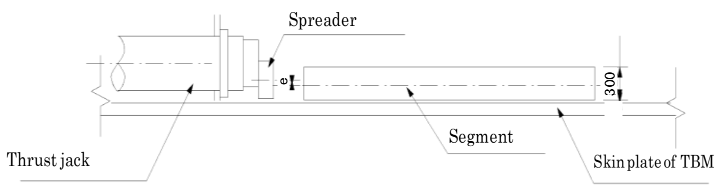

Figure 3: Ring joint of segment

from the jack thrust (P=2500kN) as a construction load as shown in Figure 3. Coefficient of soil reaction, "k", at lime stone to be set up k=10MN/m^3 as the max value of past records, because of young's module at lime stone is E=300,000kN/m^2, and Mudstone which is E=150,000ｋN/m^2.

*Soil reaction, in this case, N-value at lime stone is over 50. The coefficient of soil reaction (k) which is over 50 N-value is calculated by the following equation which is adapted from Japan Road Association, [4]

$$K_H = K_{Ho} \cdot (\frac{B_H}{0.3})^{-3/4} \div a = 1000000 \times (\frac{4.525}{0.3})^{-3/4} \div 1.3 = 100MN/m^3$$

Where, shape factor a is 1.3 and

$$B_H = \frac{D_o}{\sqrt{2}} = \frac{6.4}{\sqrt{2}} = 4.525m \qquad K_{Ho} = \alpha \cdot \frac{E_o}{0.3} = 1 \times \frac{300000}{0.3} = 1000000kN/m^3$$

As a result, the coefficient of soil reaction (k) =100MN/m^3.

6. Relationship between stress of the tensile side and strain of SFRC component

The stress-strain curve, which is usually obtained by dividing the load by original cross section, and displacement by original length, can neither be classified as perfectly elastic-brittle, nor as perfectly elastic- plastic, thus leads to utilized an elastic softening formulating [5], Figures 4 and 5 shown the tensile softening curve plots the relation between tensile stress and opening width of crack.

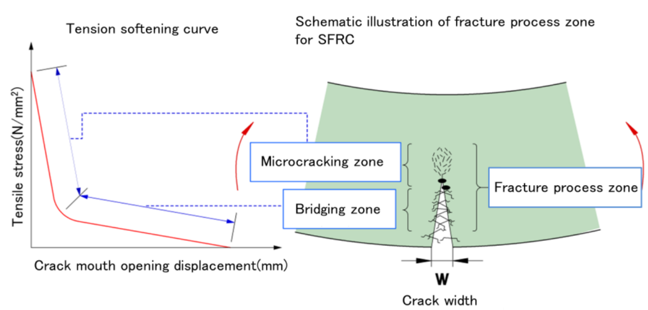

Figure 4: Fracture processing zone[5]

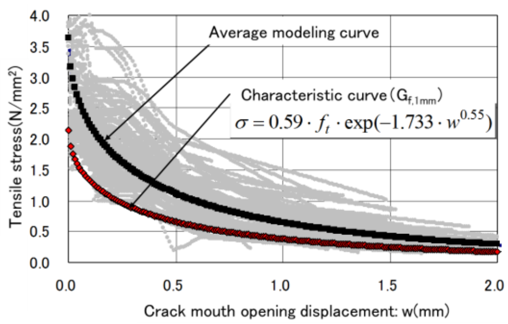

Figure 5: Tension softening curve[5]

In this design, the opening width of crack was converted to strain [6]. The conversion of tensile stress to strain is defined the proportion to Young's modulus before occasion of crack of concrete, and after occasion of crack, the relation between strain ε and the opening width of crack is defined based on equivalent length L_{eq} and converted to the relation between tensile stress and strain. Hereby, strain=ε, opening width of crack=w, and equivalent length=L_{eq} are shown as ε=w/ L_{eq}. The equivalent length L_{eq} taken as average crack spacing and it is relevant to the high, shape. Where the tensile softening curve of segment based on the curve of the Figure 4, therefore, the equivalent length L_{eg} is based on the curve of the Figure 6 [6]. With the height of segemnt equal to 300mm, the L_{eg}/h= 1.31, this value will be used in the following equation to check the maxium allowabe strain not be cxceed to ultimate strain of concrete which is ε = 0.002 as shown in the Figure 7 [6].

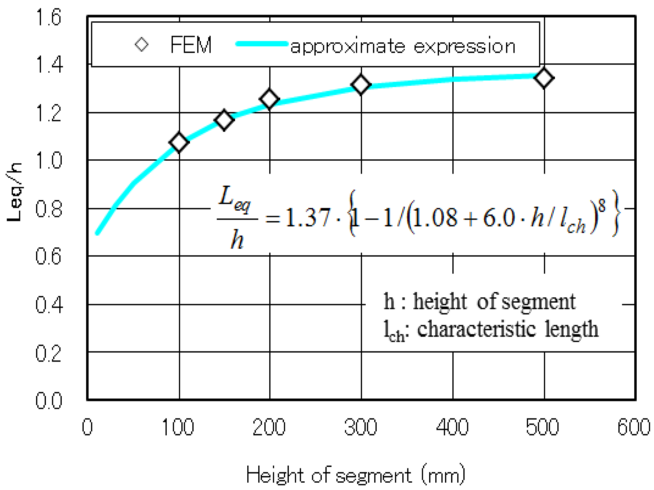

Figure 6: Relationship between height of segment and L_{eq}[6]

$$\varepsilon = \frac{\delta}{E_c} \quad \varepsilon \le \varepsilon_{cr} \quad \text{And,} \quad \varepsilon = \frac{f(0)}{E_c} + \frac{w}{L_{eq}} \quad \varepsilon \ge \varepsilon_{cr}$$

The relation of tensile stress and strain which was used in verification of ultimate limit state in this design is shown as Figure 7.

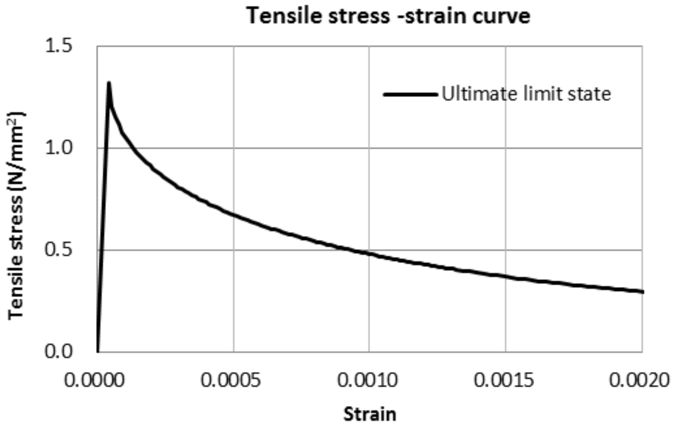

Figure 7: Actual tensile stress-strain curve

7. Design methodology for segment lining

Structural calculation in the transverse direction of segment lining is assumed to the Beam-spring model as shown Figure 8. The Beam-spring method has a current method and features for calculating member forces as follows:

- Reasonable modeling of the performance of staggered arrangement using rotational rigidity for segment joints and shear rigidity for ring joints
- Modeling of realistic behavior is possible compared to the other calculation method.
- Member forces at ring joints can be obtained from this pseudo three-dimensional analysis.

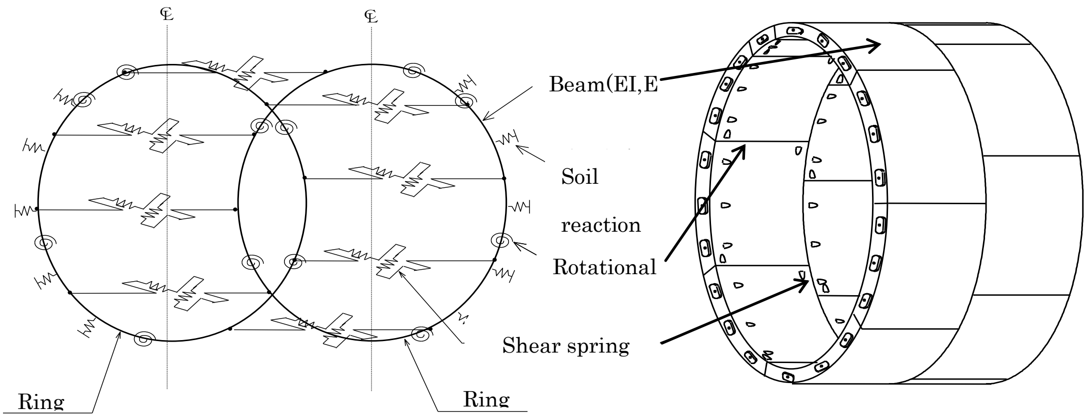

Figure 8: Beam-spring Model (Joint stiffness reduced)

Design condition of Segment lining

E	: elastic modulus of segment (kN/m^2)
I	: moment of inertia of segment (m^4)
A	: area of cross section of segment (m^2)
kθ	: rotational spring between segment pieces
ksr	: radial shear spring between segment rings
kst	: tangential shear spring between segment rings
k	: coefficient of sub grade reaction

8. Rotational spring constant between segments

Figure 9 shows the rotational spring constant model with inclined bolt between segments is calculated based on the theoretical equation for concrete coupling [7].

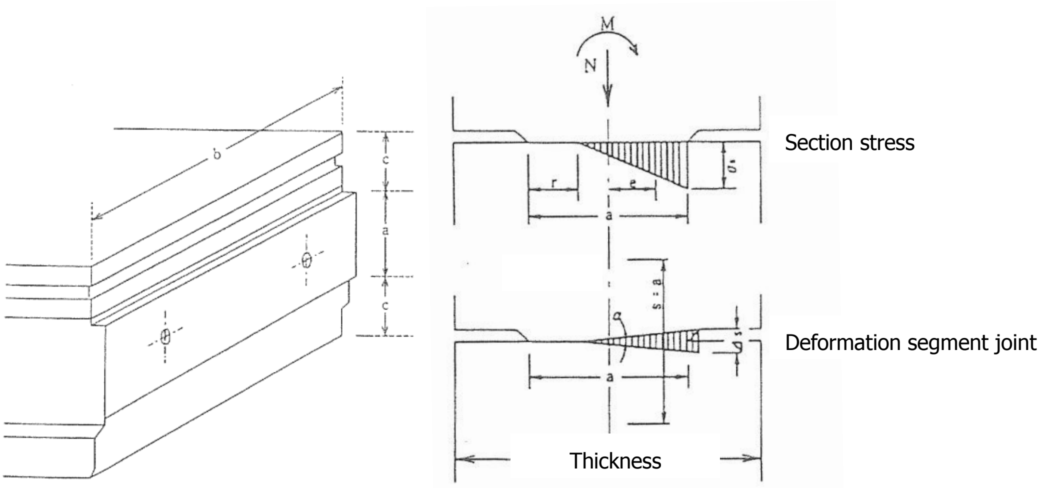

Figure 9: Model of segment joint as concrete joint

$$K_\theta = \frac{9a^2 \cdot b \cdot E_C}{8} m(1-2m)^2$$

Where,
K_θ: Rotational spring constant (kN·m/rad), a: Width of coupling contact surface (m) 0.140
Ec: Modulus of elasticity of concrete (kN/m^2) 3.15×10^7
m:=Mj / (Nj·a) Eccentricity rate, Mj: Bending Moment of coupling (kN·m)
Nj: Axial force of coupling (kN)

9. Verification items

Table 2 gathers all items that must be verified before allowing to apply the SFRC in lining tunnel in the project.

Table 2: Check points at the ultimate and serviceability limit state

	Part	Action force	Limit state
Ultimate limit state	Segment body	Axial force and/or Bending moment	1) Acting axial force only, compressive stress at the compression gets to the ultimate compressive strain of SFRC member 2) Acting axial force and bending moment - Depth of cracks is under 0.7h, - Depth of cracks gets to 0.7h Where "h" represents height of the member.
	Ring joint	Shear force	Shear capacity at shear plane of concrete.
	Segment joint	Axial force	Splitting stress (tensile stress) caused by axial force get to the tensile strength of SFRC member.
Serviceability limit state	Segment body	Axial force and/or bending moment	Compressive stress of SFRC member shall be limited not to exceed $0.4f'_{ck}$. Tensile stress of SFRC shall be limited not to exceed flexural cracking strength.
	Segment joint	Axial force and/or bending moment	Compressive stress of concrete shall be limited not to exceed 0.4f'ck. *

10. Input data

Table 3 shows the all input data with the applied safety factor, for the ultimate limit state and serviceability limit sate.

Table 3: Input data

Items	Symbol Unit	Input Data					
		Ultimate Limit State			Serviceability Limit State		
		Main value	Safety Factor	Applied value	Main value	Safety Factor	Applied value
Elastic Modulus of Segment	E kN/m^2	3.15×10^7	--	3.15×10^7	3.15×10^7	--	3.15×10^7
Area of Cross Section of Segment	A m^2	0.45	--	0.45	0.45	--	0.45
Moment of Inertia of Segment	I m^4	3.375×10^{-3}	--	3.375×10^{-3}	3.375×10^{-3}	--	3.375×10^{-3}
Diameter of central line of Segment	Dc m	3.05	--	3.05	3.05	--	3.05
Rotational Spring Value	k_θ kN X m/rad	63,100 33,900 0	--	63,100 33,900 0	63,100 33,900 0	--	63,100 33,900 0
Radial shear spring between segment rings	k_r kN/m/Ring	34,500	--	34,500	34,500	--	34,500
Tangential shear spring between segment rings	k_t kN/m/Ring	0	--	0	0	--	0
Vertical earth pressure	p_{vc} kN/m/Ring	124.32	1.0	124.32	124.32	1.0	124.32
Lateral earth pressure at tunnel crown	q_{e1} kN/m/Ring	44.47	1.0	44.47	44.47	1.0	44.47
Lateral earth pressure at tunnel bottom	q_{e2} kN/m/Ring	86.00	1.0	86.00	86.00	1.0	86.00
Water pressure at tunnel crown	p_{w1} kN/m/Ring	281.55	0.9	253.40	281.55	1.0	281.55
Water pressure at tunnel bottom	p_{w2} kN/m^2/Ring	373.05	0.9	33.75	373.05	1.0	373.05
Dead weight	g_1 KN	11.70	1.0	11.70	11.70	1.0	11.70
Coefficient of subgrade reaction	k kN/m/Ring	150000	0.9	135000	150000	1.0	150000
Coefficient of lateral earth pressure	λ kN/m/Ring	0.35	1.0	0.35	0.35	1.0	0.35

11. Result of verification at ultimate limit state

The result of verification of the flexural capacity of main part of segment of an ultimate limit state is shown in Figure 10, as well as from the data in the Table 3, it is clear that the value obtained by multiplying the ratio of the structure factor to the design force is not greater than 1.0, therefore, it is confirmed that tunnel lining for Greater Cairo Metro Line No.4 can be satisfied by the SFRC instead of normal steel reinforcements.

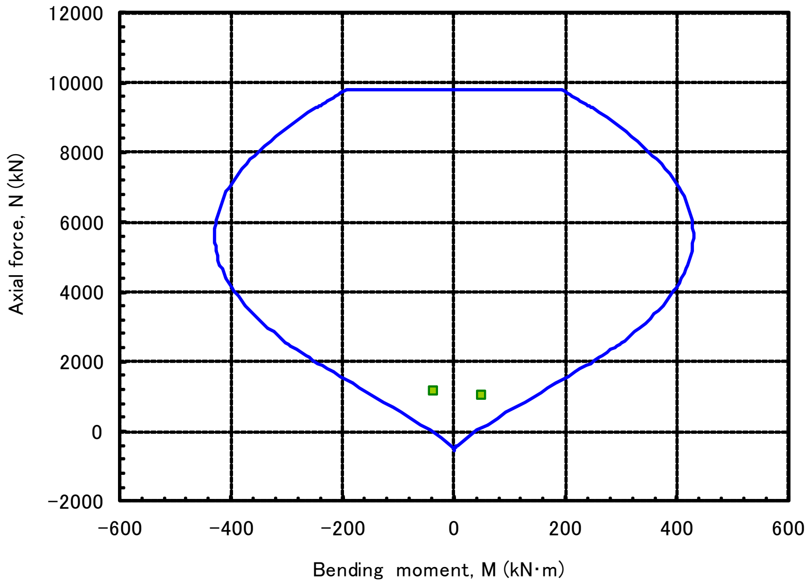

Figure 10: Bending moment and axial force diagram in ultimate limit state

Table 3: Result of reviews of segment body in ultimate limit state

Positive bending moment	Design bending moment, M_d	kN×m	38.22
	Design axial force, N'_d	kN	1092.69
	Structure factor, γ_i	-	1.2
	$\gamma_i \times M_d$	kN×m	45.86
	Ultimate moment, Mud	kN×m	152.224
	Result, $\gamma_i \times M_d/M_{ud}<1$		0.30 O.K.
Negative bending moment	Design bending moment, M_d	kN×m	-33.73
	Design axial force, N'_d	kN	1214.73
	Structure factor, γ_i	-	1.2
	$\gamma_i \times M_d$	kN×m	-40.48
	Ultimate moment, M_{ud}	kN×m	165.310
	Result, $\gamma_i \times M_d/M_{ud}<1$		0.24

12. Result of verification at serviceability limit state

Verification is carried out by the confirmation that cracks the serviceability limit state are below generating flexural capacity by drawing of N-M interaction curve. N-M interaction curve is shown in. Figure 11, the verification result at serviceability limit state is shown in Table 4.

However, considering the accident such as dropping of segment, the minimum reinforcement bar shall be installed in SFRC segment lining.

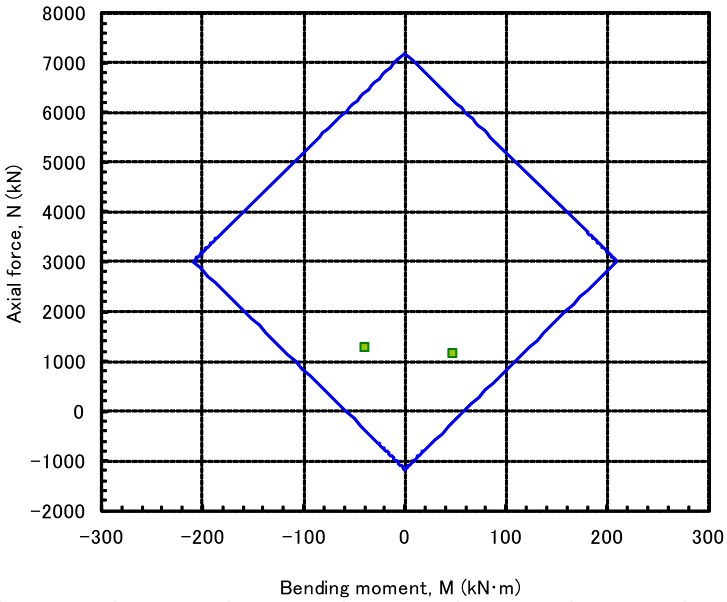

Figure 11: Bending moment and axial force diagram of segment body in serviceability limit state

Table 4: Result of review of segment body in serviceability limit state

Positive bending moment	Design bending moment, M_d	kN ×m	37.72
	Design axial force, N'_d	kN	1179.52
	Structure factor, γ_i	-	1.0
	$\gamma_i \times M_d$	kN×m	37.72
	Bending moment, M_{sd}	kN×m	117.57
	Result, $\gamma \times M_d/M_{sd}<1$		0.32 O.K.
Negative bending moment	Design bending moment, M_d	kN×m	-34.62
	Design axial force, N'_d	kN	1301.70
	Structure factor, γ_i	-	1.0
	$\gamma_i \times M_d$	kN×m	34.62
	Bending moment, M_{sd}	kN×m	123.68
	Result, $\gamma_i \times M_d/M_{sd}<1$		0.28 O.K.

13. Deformation of segment ring

The deformation of segment rings is less than D/200 by high margin of factor of safety. The vlues are gathered in Table 5.

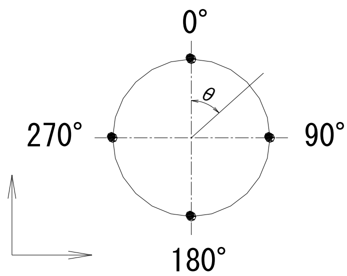

Table 5: Result of the review of examination for deformation of segment rings

Inner area deformation		Unit	Value
Maximum deformation	θ	(°)	2.81 – 182.81
	ΔD	(mm)	-2.3
Vertical deformation	0°	(mm)	-1.8
	180°	(mm)	0.5
	Total	(mm)	2.3
Horizontal deformation	90°	(mm)	0.4
	270°	(mm)	-0.4
	Total	(mm)	0.8
Maximum Permissible deformation	D/200	(mm)	32.0
Result			OK

14. Summary of the results

The design service life is designed to be 100 years, and the shield segment require to maintain their function without maintenance during the service life, to achieve this, it is required to adopt maintenance free, even if initial construction costs rise due to material price, the final life cycle cost (LCC) can be reduced by eliminating the necessity of coating, however the price of production one segment with steel fiber in the local market in Egypt same as steel reinforcement, moreover, steel fiber provide a resistance to stress in all directions and as the steel fibers present close to the surface, ensure excellent reinforcement at the joints of the segments, furthermore, steel fiber provide a substantial increase in load capacity to first cracks and the joint also good control of shrinkage cracks, as well as, steel fibers prevent a crack from growing by transferring the tension across the crack.
At the construction stage, it is expected to achieve the piratical advantage such as increase productivity in the precast operation by about 10%. Eliminate fabrication storage and positioning of reinforcement cages, no increase in batch mixing time; reduce the repaired and rejected segments.

Table 6: Summary of safety verification for the SFRC Segmental lining

Ultimate limit state	Segment Body	Flexural capacity	$\gamma_i \times M_d/M_{ud}<1$	0.30
	Segment Joint	Splitting capacity	$\gamma_i \sigma_{td}/(f_{td}/\gamma_b)<1$	0.69
		Bearing capacity	$\gamma_i \times \gamma_b \times N'd/F<1$	0.28
	Ring Joint	Shearing capacity (concave section)	$\gamma_i \times S_d/V_{cd} < 1$	0.01
		Shearing capacity (convex section)	γ_i x $S_{jd}/V_{cwd}<1$	0.04
Serviceability limit state	Segment Body	Deformation	<32.0 mm	2.3 mm

15. References

1- National Authority for Tunnels, Geotechnical Investigation Report, Greater Cairo Metro - Line No. 4, Egypt, 2012.
2- Japanese Industrial Standards (G 3505), Non-alloy steel wire rod for conversion to wire-Part 2: Specific requirements for general purpose wire rod. Japan, 2013.
3- Standard Specifications for Tunneling-:Shield Tunnels, Japan Society of Civil Engineer. Japan, 2006.
4- Specifications for Highway Bridges Part IV Substructures, Japan Road Association, Japan, 2005.
5- Bazan, Z.P. and Oh, B. H. Crack bond theory for fracture of concrete, Rilem Mater, Construct., Paris, 1983.
6- Technical evaluation report of "A design and fabrication method of Steel Fibre Reinforced concrete segment", Japan Society of Civil Engineers (JSCE), 2010.
7- Tunnel Lining Design Report, SFRC 10, Steel Fibre Reinforced Concrete Segment, Section 10: 17km960m Tunnel through the Lime Stone Section, NAT, Egypt, 2013.
8- F. Leonhardt and H. Reimann: Betongelenke, Der Bauingenieur, 41, pp.49-56, 1966, Germany.
9- Tunnels with in-Situ Pressed Concrete Lining Author: Ya I. Marennyi,Ryszard B. Zeidler (Editor) Publisher: Ashgate Publishing Company, 1997, Madrid.
10- Waal, R.GA. de. Thrust Jack forces on a tunneling. Stevin report 25.5-97-10, 1996, Deft University of technology in Dutch, Germany.